Electronic Supplementary Material (ESI) for Physical Chemistry Chemical Physics.

Supporting information

Downplaying the role of water in the rheological changes of conducting polymers by using water-in-salt electrolytes

Thiago T. Obana, Marina M. Leite, Vitor L. Martins and Roberto M. Torresi

Departamento Química Fundamental, Instituto de Química, Universidade de São Paulo, Av. Prof. Lineu Prestes 748, 05508-000 São Paulo, SP, Brazil

1. The Sauerbrey equation and viscoelastic modelling

First published in 1959 by G. Sauerbrey,[1] the equation calculates mass changes over QCM sensor, by a linear correlation with resonance frequency changes. It is valid when a thin, homogeneous and acoustically rigid adhering mass layer covers the crystal quartz sensor. Such layers are labelled rigid films. For multi-harmonic frequency change systems, the Sauerbrey equation is valid when all the monitored normalized harmonics changes (Δf_n /n) overlap, *i.e.* the change in frequency is the same in all measured overtones (n), and the film dissipation changes are negligible. It is written as follow.[2]

$$\frac{\Delta f_n}{n} = -\frac{2(f_o)^2}{A(\mu_q \rho_q)^{0.5}}\Delta m \qquad \text{(S1)}$$

Δf_n is the resonance harmonic change and the corresponding overtone, n. Δm / A is the areal specific mass change (A = 0.785 cm^2), f_o is the crystal quartz

fundamental resonance frequency (5 MHz for Q-Sense sensor), μ_q and ρ_q are the corresponding shear modulus and density, respectively. Once those last parameters are inherent to crystal quartz, the factor $2f_o / (\mu_q\mu_q)^{0.5}$ is called crystal constant (C), which is 17.7 ng cm^{-2} Hz^{-1}.

Sauerbrey equation loses the validity when the coating film's mechanical properties start to influence crystal resonance frequency. The film is no longer rigid, it turns viscoelastic. That regime is detected when a film over QCM sensor presents expressive dissipation changes and the different normalized harmonic changes do not overlap.[3] In that case, for mass changes calculations the so-called acoustic/viscoelastic modelling is required. Herein the extended Kevin-Voigt model as proposed by Voinova[4] was accessed and implemented by the commercial software QTools (Biolin Scientific AB, Sweden). The model describes the frequency and dissipation changes as a function film viscosity (η) and shear modulus (μ)

$$\Delta f \approx -\frac{1}{2\pi h_q \rho_q}\left\{\frac{\eta_3}{\delta_3} + \sum_{i=1,2}\left[2\pi f h_i \rho_i - 2h_i\left(\frac{\eta_3}{\delta_3}\right)^2 \frac{\eta_i (2\pi f)^2}{\mu_i^{\,2} + \eta_i^{\,2}(2\pi f)^2}\right]\right\} \quad \text{(S2)}$$

$$\Delta D \approx -\frac{1}{2\pi h_q \rho_q}\left\{\frac{\eta_3}{\delta_3} + \sum_{i=1,2}\left[2h_i\left(\frac{\eta_3}{\delta_3}\right)^2 \frac{\eta_i 2\pi f}{\mu_i^{\,2} + \eta_i^{\,2}(2\pi f)^2}\right]\right\} \quad \text{(S3)}$$

$$\delta_3 = \sqrt{\frac{2\eta_3}{\rho_3 2\pi f}} \quad \text{(S4)}$$

In the equations S2, S3 and S4, h,ρ, η and μ correspond to thickness, density, viscosity and shear modulus for quartz, when labelled with subscript "q", and for the polymer layer, when labelled with the subscript "i". Such a model predicts the calculations for two layers over the crystal quartz. Therefore, S2 and S3 present

a summation over indices i = 1 and 2. The fluid properties are represented by subscript “3”. Mass change is calculated from ρh product. In the present work, a density of 1000 kg m^{-3} for polypyrrole was assumed, as proposed in other EQCM works, for rheological parameters computing.[5] Table S1 presents the fixed parameters employed for EQCM-D data modelling

Table S1: Fixed parameters for EQCM-D modelling

	Ppy(DBS)/Ppy(SO_4)	SiWE	WiSE
η / mPa s^{-1}	Varied	1	6.06
ρ / kg m^{-3}	1000	997	1.504
Δm	-	-	Δm calculated from S1 (Sauerbrey)

Also, in equations E2 and E3, the product $2\pi f_o \eta_i$ correspond to film loss modulus (G”),[6,7] being f_o the fundamental harmonic frequency. In this sense, those parameters were computed for PPy(SO_4) and PPy(DBS) in SiWE and WiSE, at potentiodynamic scan vertexes, corresponding to fully reduced polymer and oxidized potential. The obtained values are present in tables S2 and S3. Also, the obtained fitting for Δf_n / n and ΔD_n values and the corresponding calculated mass variations from such modelling for PPy(SO_4) and PPy(DBS) in the different electrolytes used are presented in Figure S1, S2, S3 and S4. Figure S1 and S3 show the potentiodynamic, Δf_n /n, ΔD_n and Δm profiles for PPy(SO_4) and Ppy(DBS) in alkali chloride electrolyte, respectively. Also, those figures present the amount of exchanged ionic and solvent species calculated from their corresponding mass variations, according to equations S5 and S6.[8–10]

$$\xi_{C^+} + \frac{W_{solvent}}{W_{CA}}\xi_{solvent} = \frac{\Delta m}{W_{CA}} + \frac{W_{c^+} q}{W_{CA} F} \quad \text{(S5)}$$

$$\xi_{A^+} + \frac{W_{solvent}}{W_{CA}}\xi_{solvent} = \frac{\Delta m}{W_{CA}} - \frac{W_{A^+} q}{W_{CA} F} \quad \text{(S6)}$$

In those equations, ξ, Δm, W, q and F correspond to the exchanged amount, Δm to the obtained EQCM-D mass variation, W to the molecular weight q to the charge and F to the Faraday constant. The subscripts C^+,A^- and CA correspond to cation, anion and the related salt, respectively. For calculating cation and corresponding solvent ξ values, ξ_{A^-} was considered to be 0, so ξ_{C^+} and $\xi_{solvent}$ could be calculated. To computing ξ_{A^-} and the concomitant $\xi_{solvent}$, $\xi_{C^+}$was considered to be 0.

Such equations allowed to analyze the chemical composition of conducting polymers charge compensation process.

To compare the rheological evolution for PPy(SO_4) and PPy(DBS) in SiWE and WiSE, the elastic shear modulus of polypyrrole films were computed by considering the film viscosity (η) in WiSE close to 0 (in present work η = 10^{-8} mPa s^{-1}), as proposed by Voinova.[4] In this sense, equations E2 and E3 are simplified:

$$\Delta f \sim h_1 \rho_1 \quad \text{(S6)}$$

$$\Delta D \sim \frac{h_1}{\mu_1} \quad \text{(S7)}$$

The equation S6 shows that resonance frequency change is proportional to the mass layer over the crystal sensor. This means that such mass change is

proportional to that one calculated by the Sauerbrey equation. Besides, equation E7 shows that dissipation changes are proportional to the relation of film thickness and shear modulus; The obtained adjusts for polypyrrole films in WiSE and SiWE are presented in figures S5 and S6.

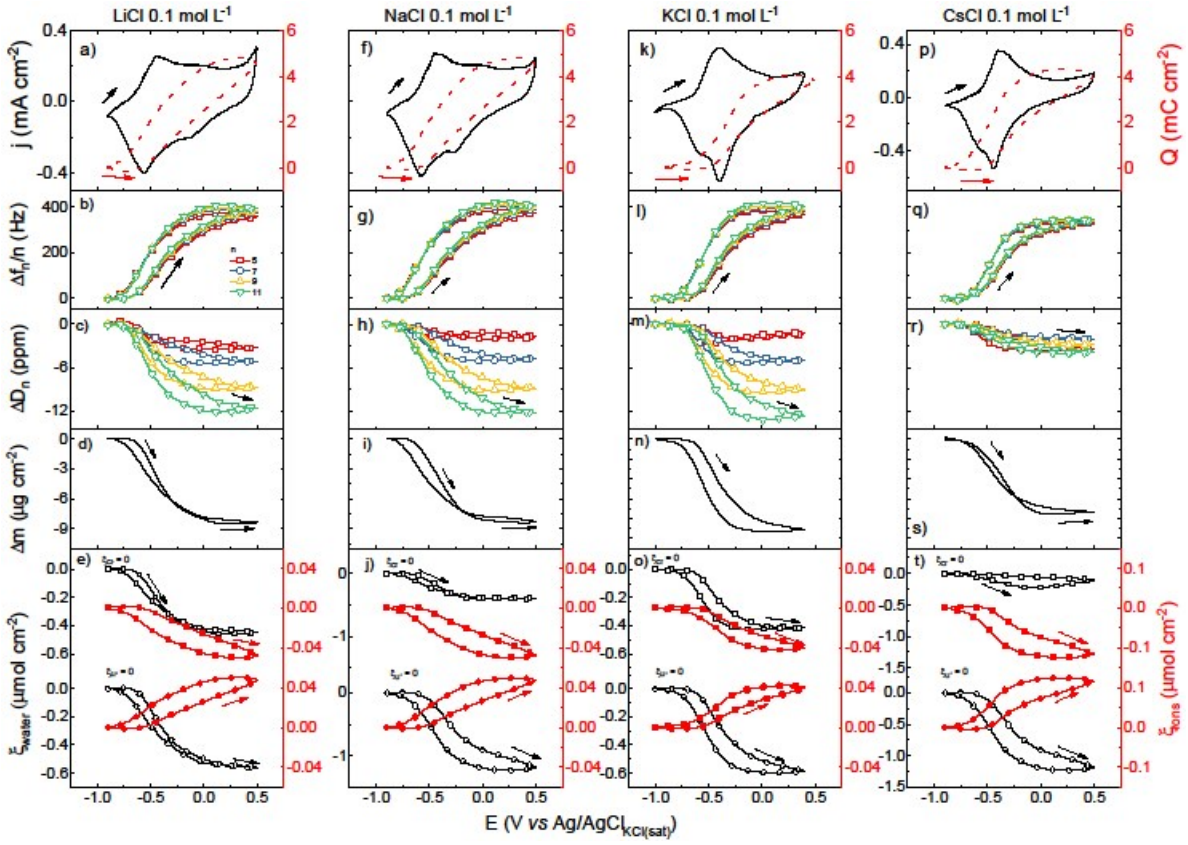

Figure S1: Potentiodynamic j-E (black full line) and Q-E (red dashed line) profiles (a,f,k,p), ($\Delta f_n/n$)-E (b,g,l,q) and ΔD_n-E profiles (c,h,m,r) at different overtones (5th red, 7th blue, 9th yellow and 11th green), modelled Δm-E profiles (d,i,n,s) and exchanged amount of ions (full red circle, anions and full red square, cations) and exchanged water molecules profiles (black open square, $\xi_{anions} = 0$ and black open circle, $\xi_{cations} = 0$) (e,j,o,t) for a PPy(DBS) in LiCl, NaCl, KCl and CsCl 0.1 mol L^{-1} from -0.9 V to 0.5V at 50mV s^{-1}.

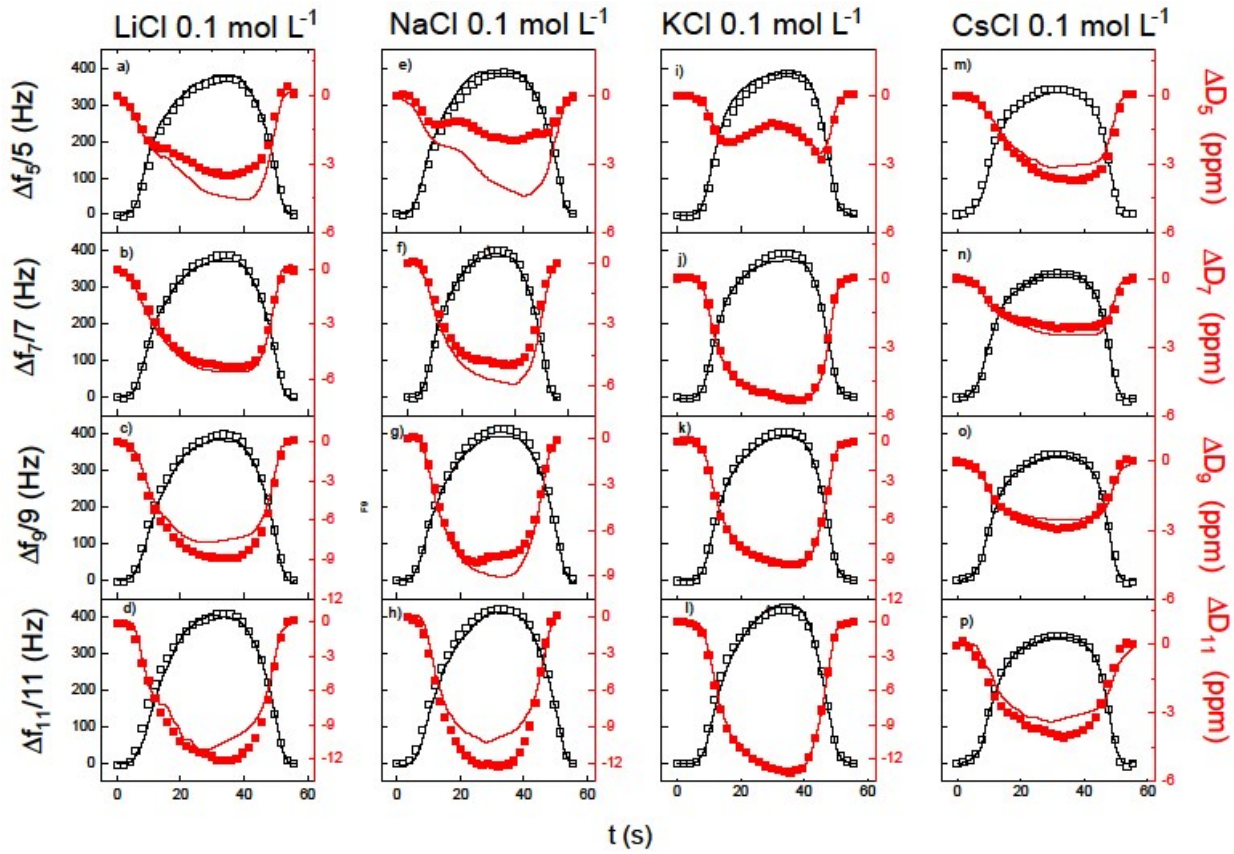

Figure S2: Experimental ($\Delta f_n/n$) – t (black open square) and ΔD_n-t (red closed square) profiles and the fitted values, black full line for $\Delta f_n/n$ and red full line for ΔD_n ones, corresponding to PPy(DBS) potentiodynamic scan (from -0.9 into 0.5 V at 50mV s^{-1}) in LiCl (a -d), NaCl (e-h), KCl (i-l) and CsCl (m-p) 0.1 mol L^{-1}.

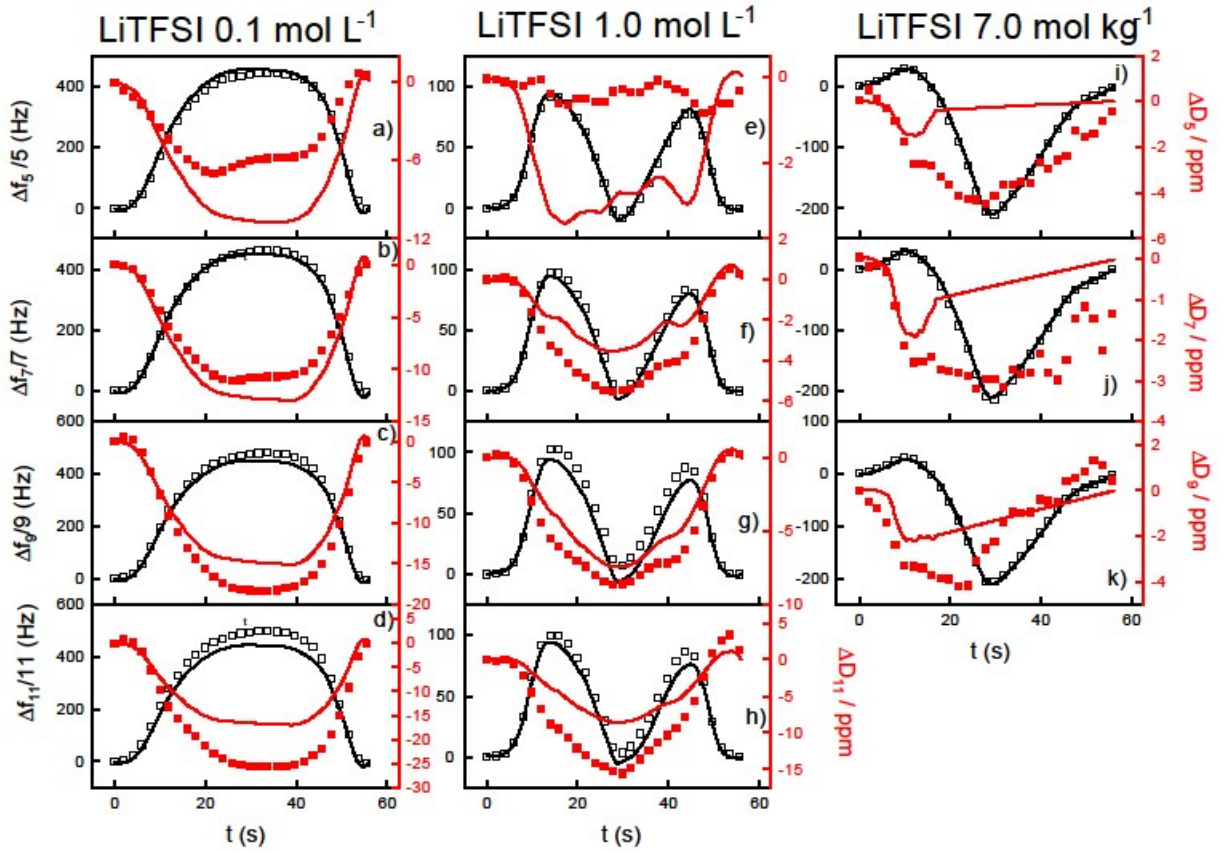

Figure S3: Experimental ($\Delta f_n/n$) – t (black open square) and ΔD_n-t (red closed square) profiles and the fitted values, black full line for $\Delta f_n/n$ and red full line for ΔD_n ones, corresponding to PPy(DBS) potentiodynamic scan (from -0.9 into 0.5 V at 50mV s^{-1}) in LiTFSI 0.1 mol L^{-1} (a -d), LiTFSI 1.0 mol L^{-1} (e-h) and LiTFSI 7.0 mol kg^{-1} (i-k).

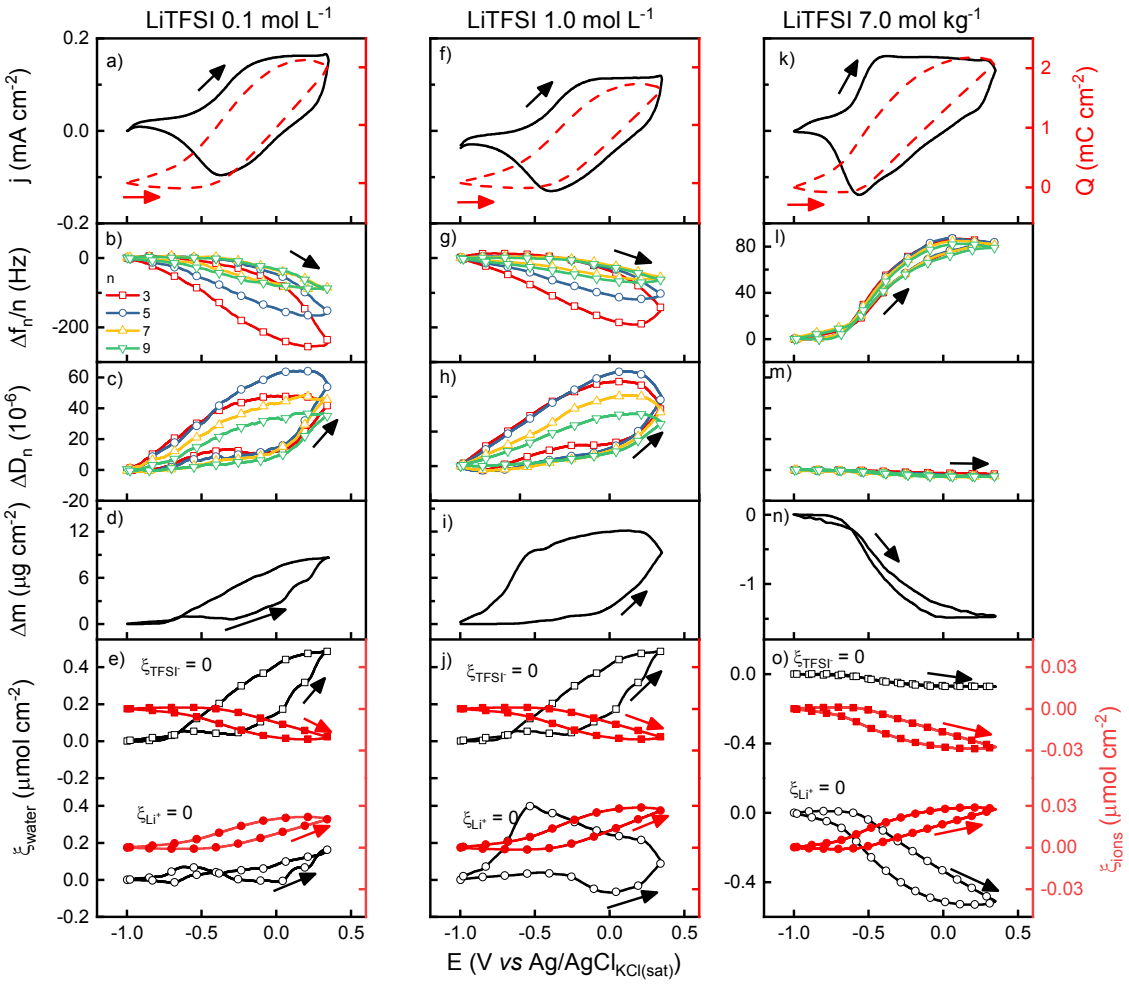

Figure S4: Potentiodynamic j-E (black full line) and Q-E (red dashed line) profiles (a, f, k), ($\Delta f_n/n$)-E (b, g, l) and ΔD_n-E profiles (c, h, m) at different overtones (3rd red squares, 5th blue circles, 7th yellow upward pointing triangles and 9th green downward pointing triangles), modeled Δm-E profiles (d, i, n) and exchanged amount of ions (full red circle, anions and full red square, cations) and exchanged water molecules profiles (black open square, $\xi_{anions} = 0$ and black open circle, $\xi_{cations} = 0$) (e, j, o) for a PPy(SO_4) film in LiTFSI 0.1 mol L^{-1}, 1.0 mol L^{-1} and 7.0 mol kg^{-1} (WiSE) electrolytes recorded at 50 mV s^{-1}.

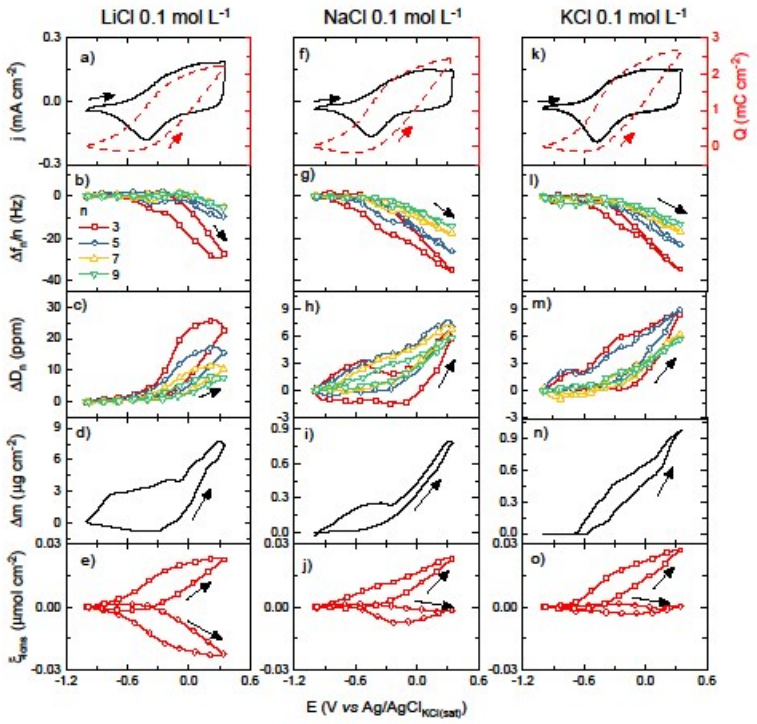

Figure S5: Potentiodynamic j-E (black full line) and Q-E (red dashed line) profiles (a,f,k), ($\Delta f_n/n$)-E (b,g,l) and ΔD_n-E profiles (c,h,m) at different overtones (3rd red, 5th blue, 7th yellow and 9th green), modelled Δm-E profiles (d,i,n) and exchanged amount of ions (open red circle, anions and open red square, cations) (e,j,o) for a PPy(SO_4) film in LiCl (a-e), NaCl(f-j) and KCl (k-o) 0.1 mol L^{-1}, from -1.0 V to 0.35V at 50mV s^{-1}.

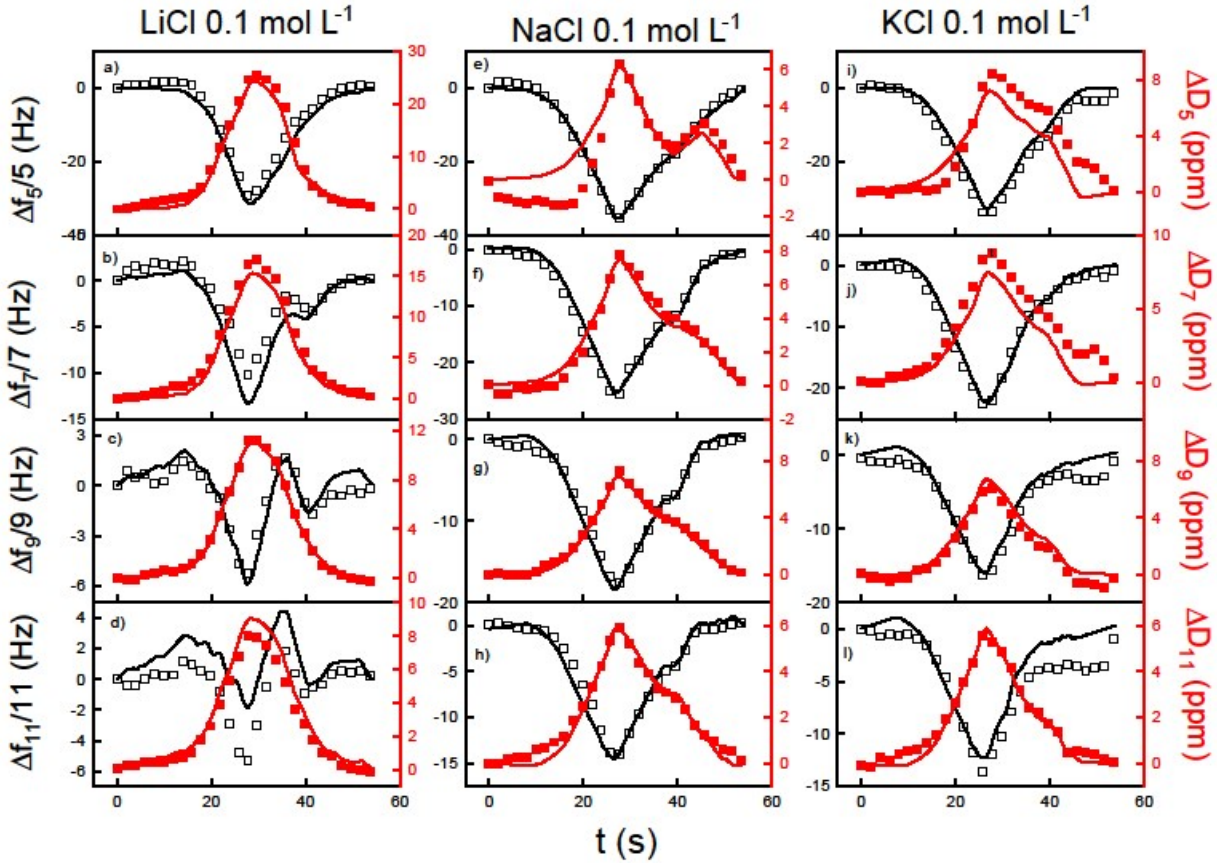

Figure S6: Experimental ($\Delta f_n/n$) – t (black open square) and ΔD_n-t (red closed square) profiles and the fitted values, black full line for $\Delta f_n/n$ and red full line for ΔD_n ones, corresponding to $PPy(SO_4)$ potentiodynamic scan (from -1.0 V to 0.35V at 50mV s^{-1}) in LiCl (a -d), NaCl (e-h) and KCl (i-l) 0.1 mol L^{-1}.

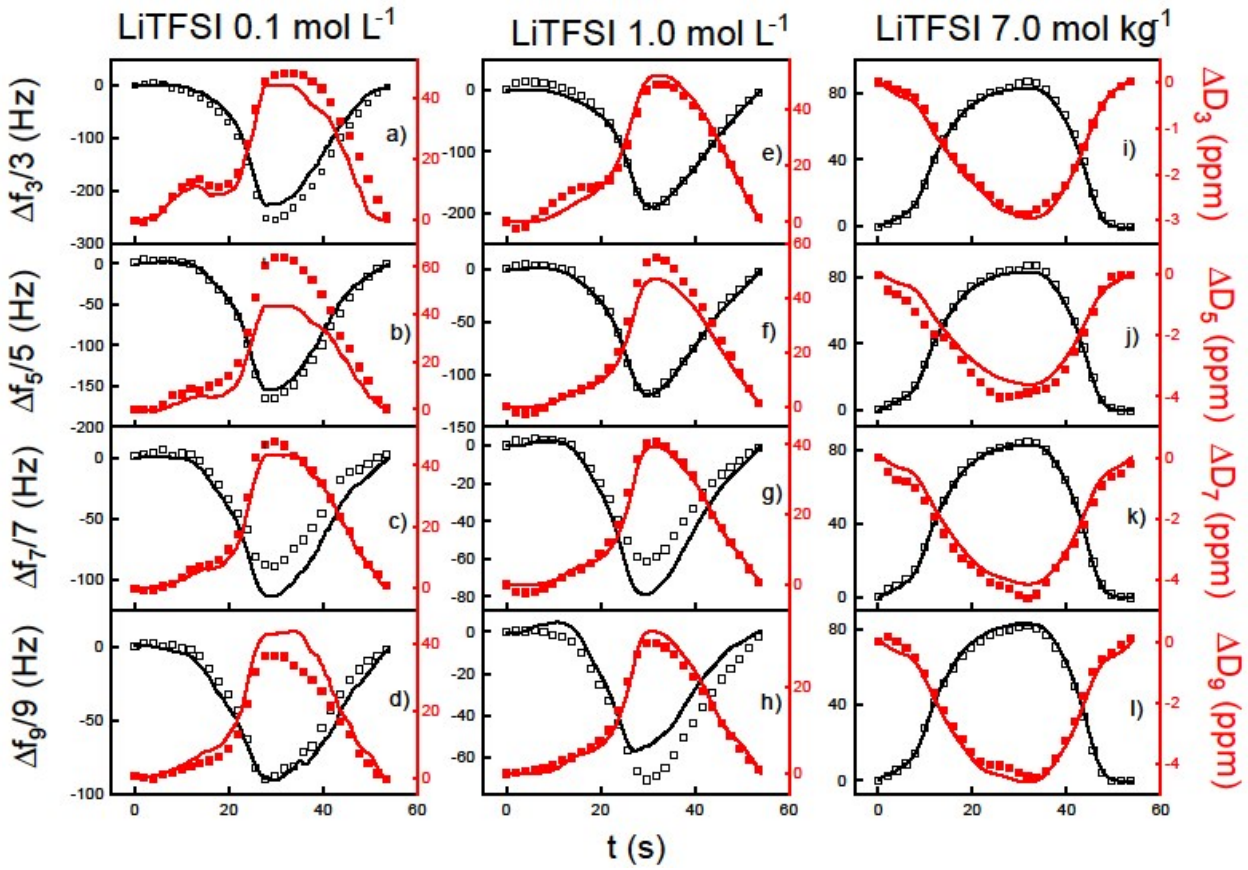

Figure S7: Experimental ($\Delta f_n/n$) – t (black open square) and ΔD_n-t (red closed square) profiles and the fitted values, black full line for $\Delta f_n/n$ and red full line for ΔD_n ones, corresponding to PPy(SO_4) potentiodynamic scan (starting from -1.0 V into 0.35V at 50mV s^{-1}) in LiTFSI 0.1 mol L^{-1} (a -d), LiTFSI 1.0 mol L^{-1} (e-h) and LiTFSI 7.0 mol kg^{-1} (i-l).

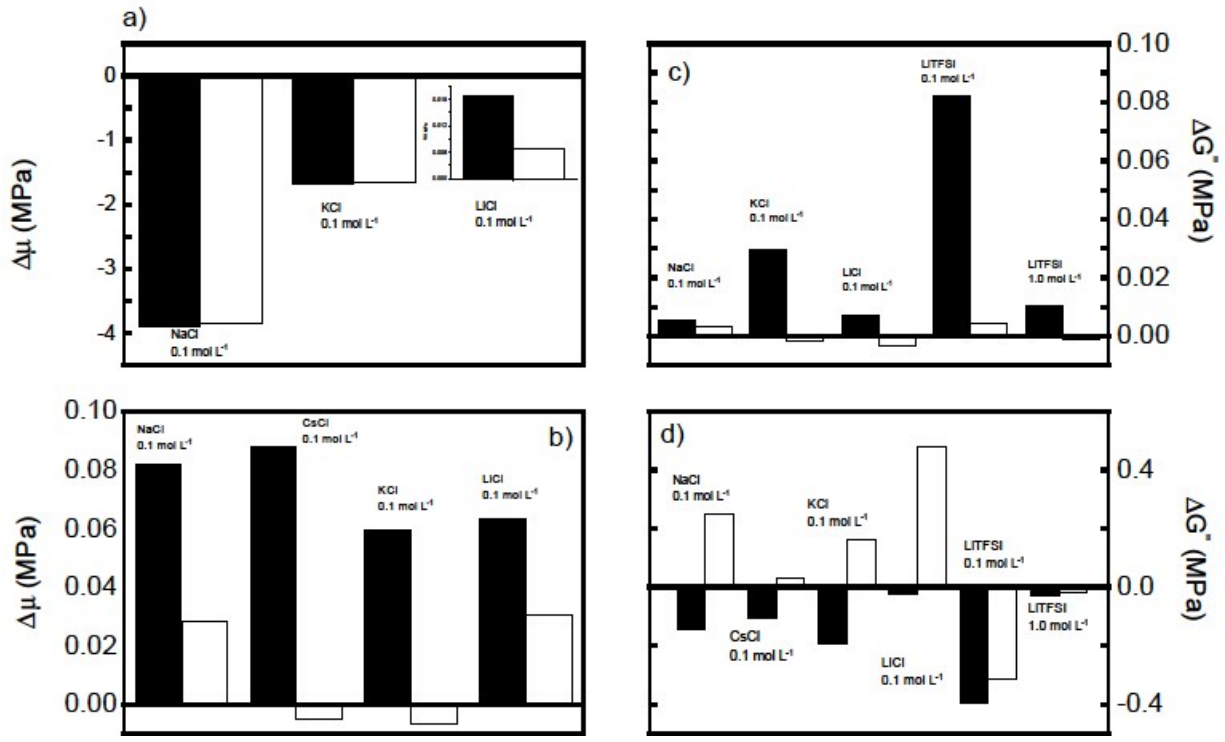

Figure S8: Variations in shear modulus (Δμ) and loss modulus ($\Delta G''$) for $PPy(SO_4)$ (a-b) and of PPy(DBS) (c-d) film in LiCl, NaCl, KCl, CsCl and LiTFSI 0.1 mol L^{-1}. White columns correspond to $\mu_{oxidized} - \mu_{reduced\ initial}$ or $G''_{oxidized} - G''_{reduced}$ and black columns correspond to $\mu_{reduced\ final} - \mu_{reduced\ initial}$ or $G''_{reduced,\ final} - G''_{reduced\ initial}$.

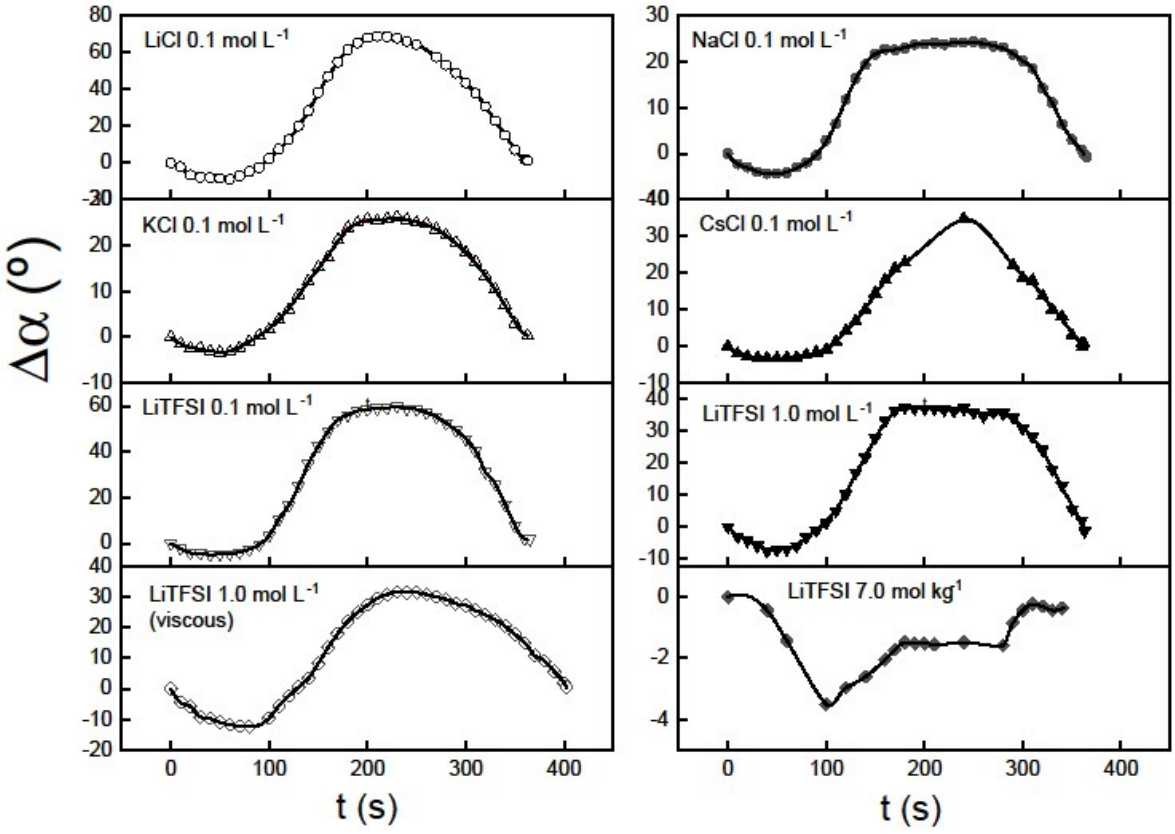

Figure S9: Measured angular displacement (symbol) and corresponding interpolation curve (black continuous line) for PPy(DBS)/tape electrode in 0.1 mol L^{-1} electrolyte: LiCl (black open circle), NaCl (black closed circle), KCl(black open triangle), CsCl (black closed triangle) and LiTFSI (black inverted open triangle), LiTFSI 1.0 mol L^{-1} (black closed inverted triangle), viscous LiTFSI 1.0 mol L^{-1} (black open diamond) and LiTFSI 7.0 mol kg^{-1} (black closed diamond).

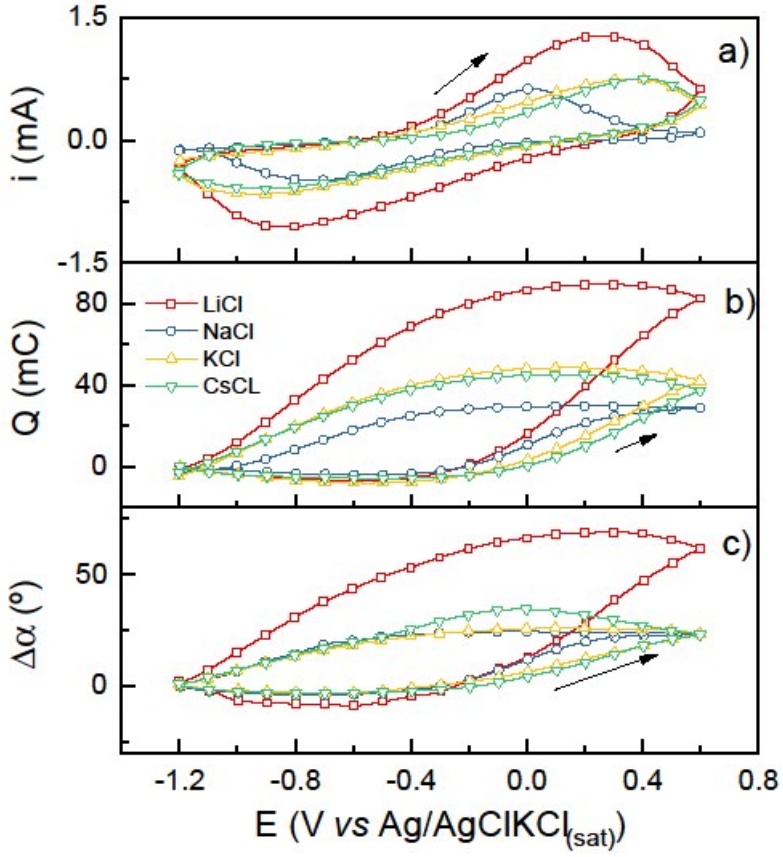

Figure S10: Potentiodynamics j-E (a), charge Q-E (b) and angular displacement Δα-E (c) profiles and for PPy(DBS) films in for PPy(DBS) films in LiCl (red open square), NaCl (blue open circle), KCl (yellow open triangle), CsCl 0.1 mol L^{-1} (green open inverted triangle), at 10 mV s^{-1}, from -1.2 to -0.6 V . The film mass for each experiment was 1,56 mg for NaCl and 1,28 mg for other 0.1 mol L^{-1} alkali chlorides. Data taken from recorded videos also available as SI.

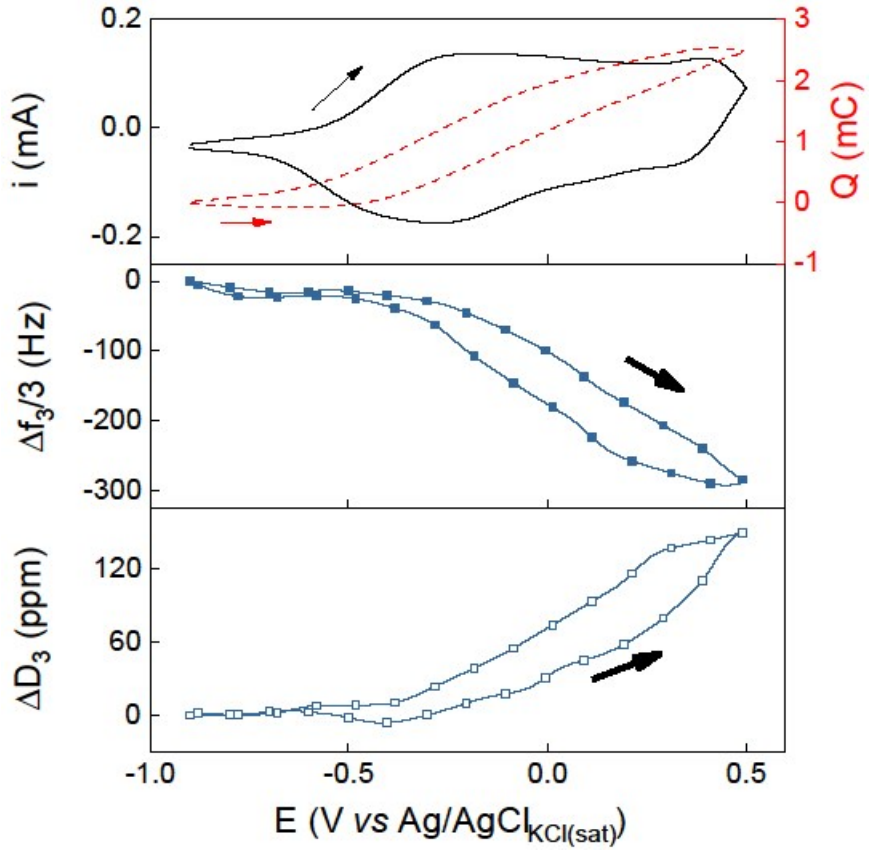

Figure S11: Potentiodynamic i-E (black full line) and Q-E (red dashed line) profiles, ($\Delta f_n/n$)-E and ΔD_n-E profiles at 3rd overtone for a PPy(SO_4) film in viscous (η = 7.11 mPa s^{-1}) LiTFSI 1.0 mol L^{-1} , from -0.9 into 0.5 V at 50 mV s^{-1}

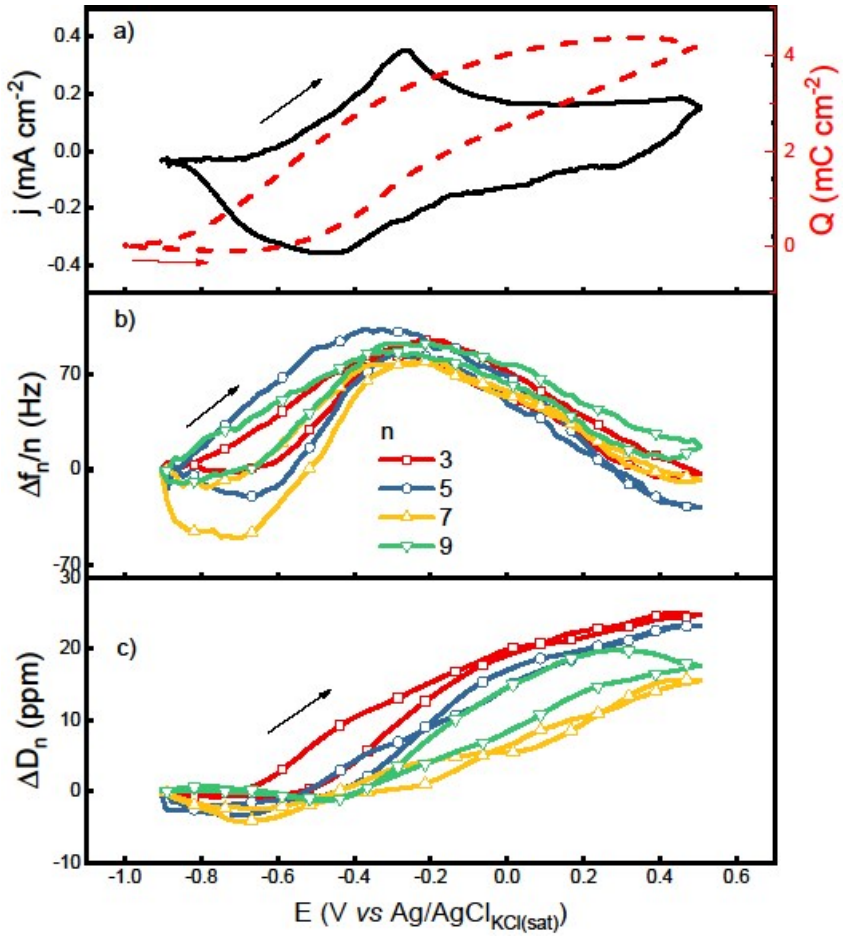

Figure S12: Potentiodynamic j-E (black full line) and Q-E (red dashed line) profiles (a), ($\Delta f_n/n$)-E (b) and ΔD_n-E profiles (c) at different overtones (3rd red, 5th blue, 7th yellow and 9th green), for a PPy(DBS) film viscous in viscous (η = 7.11 mPa s^{-1}) LiTFSI 1.0 mol L^{-1} from -0.9 into 0.5 V at 50 mV s^{-1}.

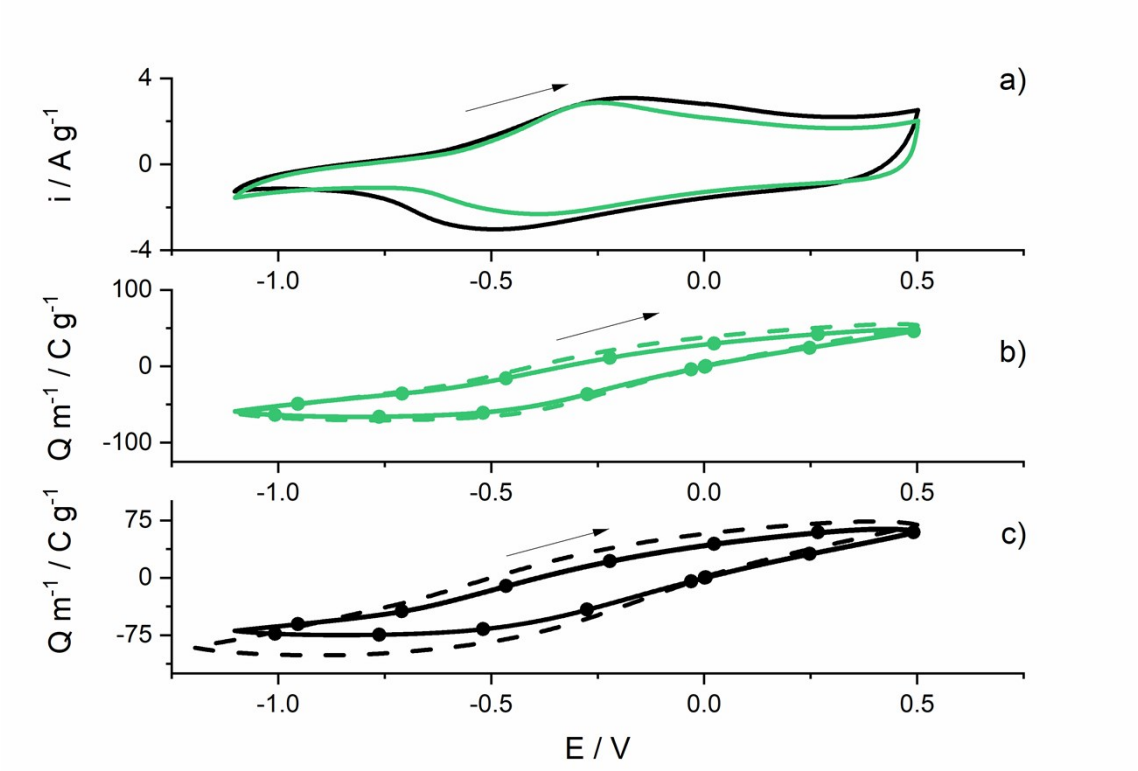

Figure S13: a) 15th potentiodynamic profile i-E for PPy(DBS)/AC cell in LiTFSI 1.0 mol L^{-1}(black full line) and in 7.0 mol kg^{-1} LiTFSI WiSE (green full line) at 20 mV^{-1} , b)PPy(DBS)/AC cell specific consumed charge as function of swept potential for 1st (dashed line), 14th (closed circles) and 15th (full line) scan related to 7.0 mol kg^{-1} LiTFSI-WiSE (green colour) and for c) LiTFSI 1.0 mol L^{-1}(black colour)

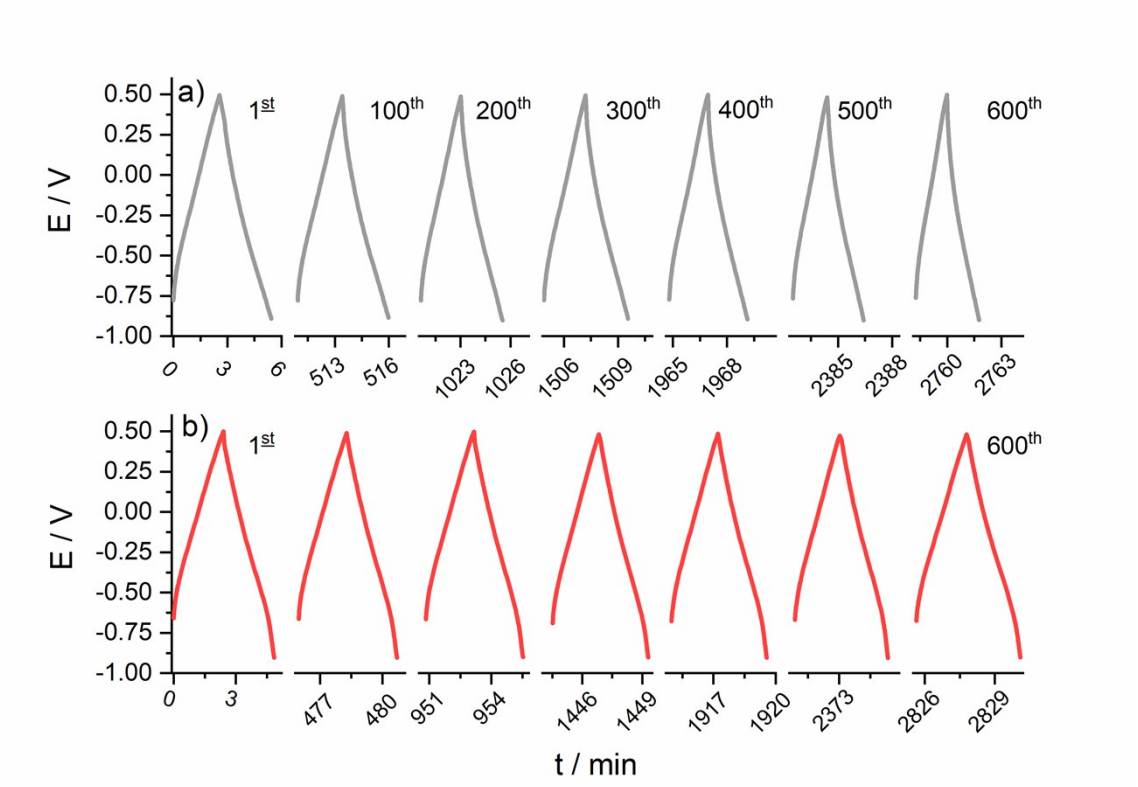

Figure S14: Galvanostatic charge-discharge curves at 0.5 A g^{-1} a) for PPy(DBS)/AC upon 600 cycles in LiTFSI 1.0 mol L^{-1} (a) and b) in 7.0 mol kg^{-1} LiTFSI (b)

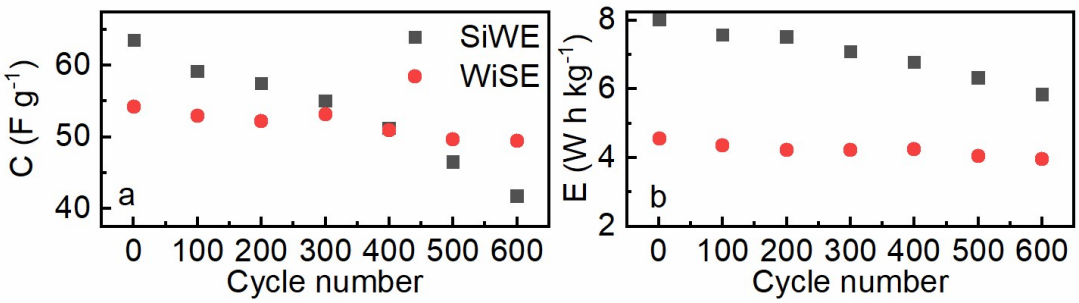

Figure S15: PPy(DBS)/AC cell specific capacitante (a) and average energy density (b),obtained from galvanostatic discharging at 0.5 A g^{-1}, in LiTFSI 1.0 mol L^{-1}(black closed squares) and in 7.0 mol kg^{-1} LiTFSI WiSE (red closed cycles) as a function of cycle number, both were normalized by PPy(DBS) mass (1,2 mg and 1,68mg for LiTFSI SiWE and LiTFSI WiSE cell, respectively).

Table S2 Rheological parameters for PPy(DBS) in fully reduced, oxidized and re-reduced state at worked electrolytes.

	Reduced			Oxidized			Reduced		
	μ / MPa	η / MPa s^{-1}	G" / MPa	μ / MPa	η / MPa s^{-1}	G" / MPa	μ / MPa	η / MPa s^{-1}	G" / MPa
NaCl	0.03	12	0.38	0.11	7.44	0.23	0.057	20	0.628
KCl	0.049	14.12	0.44	0.11	7.9	0.25	0.042	19.42	0.61
CsCl	0.015	8	0.25	0.10	4.67	0.15	0.01	9	0.28
LiCl	0.009	4.79	0.15	0.072	4.01	0.12	0.039	20.02	0.63
LiTFSI 0.1 M	0.11	25.01	0.78	0.34	12.44	0.39	0.19	15	0.47
LiTFSI 1.0 M	0.11	7.79	0.24	1.37	6.87	0.21	0.69	7.19	0.22
LiTFSI 7m	104			1000			221		

Table S3 Rheological parameters for PPy(SO_4) in fully reduced, oxidized and re-reduced state at worked electrolytes.

	Reduced			Oxidized			Reduced		
	μ / MPa	η / MPa s^{-1}	G" / MPa	μ / MPa	η / MPa s^{-1}	G" / MPa	μ / MPa	η / MPa s^{-1}	G" / MPa
NaCl	4.2	1.1	0.034	0.31	1.27	0.04	0.35	1.2	0.037
KCl	1.81	1.25	0.039	0.12	2.2	0.069	0.15	1.2	0.038
CsCl									
LiCl	0.15	1.1	0.034	0.0095	1.32	0.0414	0.034	1	0.031
LiTFSI 0.1 M	0.057	1.06	0.034	0.021	3.68	0.11	0.09	1.2	0.038
LiTFSI 1.0 M	0.099	1.95	0.06	0.025	2.28	0.072	0.024	1.91	0.06
LiTFSI 7m	4.5			5.11			5.5		

References

(1) Sauerbrey, G. Verwendung von Schwingquarzen Zur Wägung Dünner Schichten Und Zur Mikrowägung. *Zeitschrift für Phys.* **1959**, *155* (2), 206–222. https://doi.org/10.1007/BF01337937.

(2) Antonio, J. L. S.; Martins, V. L.; Córdoba de Torresi, S. I.; Torresi, R. M. QCM-D Study of Electrochemical Synthesis of 3D Polypyrrole Thin Films for Negative Electrodes in Supercapacitors. *Electrochim. Acta* **2019**, *324*, 134887. https://doi.org/10.1016/j.electacta.2019.134887.

(3) Dargel, V.; Shpigel, N.; Sigalov, S.; Nayak, P.; Levi, M. D.; Daikhin, L.; Aurbach, D. In Situ Real-Time Gravimetric and Viscoelastic Probing of Surface Films Formation on Lithium Batteries Electrodes. *Nat. Commun.* **2017**, *8* (1). https://doi.org/10.1038/s41467-017-01722-x.

(4) Voinova, M. V; Rodahl, M.; Jonson, M.; Kasemo, B. Viscoelastic Acoustic Response of Layered Polymer Films at Fluid-Solid Interfaces: Continuum Mechanics Approach. *Phys. Scr.* **1999**, *59* (5), 391–396. https://doi.org/10.1238/physica.regular.059a00391.

(5) Koehler, S.; Bund, A.; Efimov, I. Shear Moduli of Anion and Cation Exchanging Polypyrrole Films. *J. Electroanal. Chem.* **2006**, *589* (1), 82–86. https://doi.org/10.1016/J.JELECHEM.2006.01.013.

(6) Benedetti, T. M.; Torresi, R. M. Rheological Changes and Kinetics of Water Uptake by Poly(Ionic Liquid)-Based Thin Films. *Langmuir* **2013**, *29* (50), 15589–15595. https://doi.org/10.1021/la4038809.

(7) Gao, W.; Sel, O.; Perrot, H. Electrochemical and Viscoelastic Evolution of Dodecyl Sulfate-Doped Polypyrrole Films during Electrochemical Cycling. *Electrochim. Acta* **2017**, *233*, 262–273.

https://doi.org/10.1016/j.electacta.2017.03.051.

(8) Maia, G.; Torresi, R. M.; Ticianelli, E. A.; Nart, F. C. Charge Compensation Dynamics in the Redox Processes of Polypyrrole-Modified Electrodes. **1996**, *3654* (96), 15910–15916. https://doi.org/10.1021/jp9607780.

(9) Torresi, R.; Córdoba De Torresi, S.; Matencio, T.; De Paoli, M. A. Ionic Exchanges in Dodecylbenzenesulfonate-Doped Polypyrrole Part II: Electrochemical Quartz Crystal Microbalance Study. *Synth. Met.* **1995**, *72* (3), 283–287.

(10) Varela, H.; Malta, M.; Torresi, R. M. Microgravimetric Study of the Influence of the Solvent on the Redox Properties of Polypyrrole Modified Electrodes. *J. Power Sources* **2001**, *92* (1–2), 50–55. https://doi.org/10.1016/S0378-7753(00)00524-3.